Research Square

Preprints are preliminary reports that have not undergone peer review.
They should not be considered conclusive, used to inform clinical practice,
or referenced by the media as validated information.

Process-level uncertainties challenge system-level direct air capture assessments

Henrik Wenzel

h.wenzel@fz-juelich.de

Forschungszentrum Jülich GmbH https://orcid.org/0000-0001-8203-4930

Malte Glaser

Department of Chemical and Petroleum Engineering, University of Calgary

Mattia Galanti

Department of Chemical Engineering and Chemistry, Eindhoven University of Technology

Tom Terlouw

Paul Scherrer Institute https://orcid.org/0000-0003-3744-9728

Daniel Rezo

Institute of Technical Thermodynamics, RWTH Aachen University

Vittoria Bolongaro

Energy and Process Systems Engineering, Institute of Energy and Process Engineering, ETH Zurich

Mak Dukan

Forschungszentrum Jülich GmbH

Aaron Jajjawi

Forschungszentrum Jülich GmbH https://orcid.org/0009-0000-0782-3083

Jochen Linßen

Forschungszentrum Jülich https://orcid.org/0000-0003-2805-2307

Niall Mac Dowell

Imperial College London https://orcid.org/0000-0001-7179-2701

Sean McCoy

University of Calgary

Russell McKenna

ETH Zurich

Ralf Peters

Forschungszentrum Jülich GmbH https://orcid.org/0000-0002-7995-7563

Thomas Schöb

Forschungszentrum Jülich GmbH, Institute of Climate and Energy Systems

Marwan Sendi

Life Cycle Assessment Group, Technology Strategy & Planning Department, Saudi Aramco

Martin van Sint Annaland

Forschungszentrum Jülich GmbH

Niklas von der Assen

RWTH Aachen University https://orcid.org/0000-0001-8855-9420

Carsten Wedler

Institute of Technical Thermodynamics, RWTH Aachen University

Christoph Winkler

Forschungszentrum Jülich GmbH

Jann Weinand

Forschungszentrum Jülich https://orcid.org/0000-0003-2948-876X

Analysis

Keywords:

Posted Date: November 2nd, 2026

DOI: https://doi.org/10.21203/rs.3.rs-11387567/v1

License: This work is licensed under a Creative Commons Attribution 4.0 International License. Read Full License

Additional Declarations: There is **NO** Competing Interest.

Abstract

System-level assessments of direct air capture (DAC) commonly rely on individual process models, overlooking the influence of model choice on system-level conclusions. Here, we quantify this impact by integrating weather-dependent performance data from seven solid-sorbent DAC models into an otherwise consistent energy system framework. DAC representation is the largest source of variation in levelized CO2 capture cost, accounting for 43% of the observed variation across the climate-renewable archetypes considered compared with 16% for climate and 6% for renewable-resource configuration. Model-dependent cost differences exceed 1000 € tCO2-1 at individual locations. Different model representations can also reverse siting preferences, substantially alter cost-optimal system design, and determine whether future CO2 capture-cost targets are achieved. Our results further demonstrate how individual process-level assumptions can propagate through the assessment, resulting in a major source of system-level uncertainty. The harmonized DAC performance data developed here enable systematic comparison of alternative DAC representation in future system assessments.

Main

Solid-sorbent direct air capture (DAC) can contribute to climate-change mitigation by removing CO_2 directly from the atmosphere. DAC plays a vital role in almost inevitable emission overshoot scenarios from integrated assessment models (IAMs)[1,2], widely used to explore mitigation pathways and inform assessments by the Intergovernmental Panel on Climate Change (IPCC). Assumptions about the costs and resource requirements of DAC can ultimately influence conclusions about the role of carbon dioxide removal in achieving climate targets[3,4]. Technology-focused system assessments of DAC are therefore becoming increasingly relevant for translating process-level characteristics into techno-economic parameters that can inform its representation in IAMs.

Early DAC assessments emerged around 2010 but were typically limited to plant-level techno-economic cost estimates and case studies[5–8]. Sendi et al.[9] later introduced spatially resolved weather effects into techno-economic DAC assessments by coupling a solid-sorbent adsorption model with hourly meteorological data to map electricity and heat demand as functions of temperature and relative humidity. Their analysis demonstrated that cold and dry climates substantially reduce DAC costs. A later extension also highlighted the influence of energy supply[10], emphasizing the need for system-level assessments with energy system or integrated assessment models. At the same time, Wiegner et al.[11] developed an alternative weather-dependent process model for DAC, likewise demonstrating the importance of ambient conditions for DAC system performance but reaching different conclusions about which climate conditions are most favorable. Since then, the number of DAC assessments has increased substantially[12–19], although only a limited number account for weather-dependent process performance of DAC and include a spatio-temporal coupling to an energy system (see Supplementary Table 1). While weather-dependent DAC performance improves on constant performance assumptions it remains specific to the underlying process model and its assumptions on design, cycle characteristics and material properties, thereby introducing a new dependency. Previous assessments have considered only a single process representation[13,18,19], leaving the robustness of reported effects of climate, siting, and system integration across alternative representations unexplored.

A qualitative comparison of existing solid-sorbent DAC process models reveals a relatively homogeneous picture at a high level (Table 1). Most solid sorbent DAC process models represent temperature-vacuum swing adsorption in packed-bed contactors using amine-functionalized sorbents, and several share common descriptions of adsorption equilibria and kinetics. Beyond these similarities, however, the models differ substantially in the experimental data used for parameterization, thermodynamic and kinetic formulations, contactor geometry and cycle characteristics (see Supplementary Information). Such differences arise even for the same sorbent: Jajjawi et al.[12], Sendi et al.[9] and Jung et al.[20] parameterize their models using Lewatit data reported by Young et al.[21], whereas Schellevis et al.[22] use on an alternative dataset from the Brilman group[23]. By considering multiple published datasets, Galanti et al.[24] reveal substantial inconsistencies in reported properties for the same sorbent. These differences are consequential because individual process parameters, including mass-transfer coefficients and isotherm formulation, can substantially affect predicted DAC performance[25], likely resulting in different estimates of energy demand and productivity. Because performance data provides the interface between process models and system-level assessments of DAC it remains unclear to what extent these differences propagate to the system-level.

Table 1: High-level comparison of existing DAC process models. A more detailed assessment with additional information on each model can be found in the Supplementary Information. Based on refs[9,11,12,15,16,20–22,24,26–34]. Abbreviations: T – Toth, GAB – Guggenheim-Anderson-de-Boer, cp – chemi-physisorption, S – Sip, L – Langmuir, WADST – Weighted Average Dual Site Toth, CATSO – Collaborative Adsorption Toth with Site Obstruction, LDF – linear driving force, (RH) – relative humidity-dependent, (T) – temperature-dependent, TVSA – temperature vacuum swing adsorption.

Study	Process	Contactor	Sorbent		Isotherms			Kinetics
			Name	Type	CO2	H2O	Co-Adsorption	
Abdullatif 2023	TVSA	n/s	Lewatit		T	GAB	Mechanistic	no
Balasubramaniam 2024	TVSA, TVSA (steam-assisted)		Multiple		T	GAB	Modified Toth	LDF
Cai 2024	TVSA		Resin			GAB	Mechanistic rate-based	LDF H2O, Rate-based CO2 (RH)
Glaser 2025	TVSA, TVSA (steam-assisted)		Multiple		T	GAB	Modified Toth	LDF
Jajjawi 2026	TVSA		Lewatit		T	GAB	WADST	LDF
Wiegner 2022	TVSA		Exemplary		T-cp	GAB	Modified Toth-cp	LDF
Sabationo 2021	TVSA		Multiple		T-cp	GAB	Modified Toth-cp	LDF
Sendi 2022	TVSA (steam-assisted)		Lewatit		T	GAB	Mechanistic	LDF
Jung 2025	TVSA		Lewatit		T	GAB	Mechanistic	LDF
Rezo 2026	TVSA		Lewatit		T	GAB	Mechanistic	LDF (T)
Postweiler 2024	TVSA, TVSA (steam-assisted)		APDES		T	GAB	Modified Toth	LDF
Schellevis 2024	TVSA (steam-assisted)	n/s	Lewatit		T	GAB	Modified Toth	LDF H2O (RH/T), Rate-based CO2 (T)
Shakouri Kalfati 2025	TVSA		Li-X, Na-X		S, L	L	Modified Langmuir	LDF (T) or local equilibrium
Ward 2024	TVSA (steam-assisted)		APDES		T	GAB	Modified Toth	LDF
Young 2021	TVSA		Lewatit		T	GAB	Mechanistic / WADST	LDF
Ferru 2026	TVSA (only steam)	Monolith	Alumina		T	GAB	CATSO	LDF
Galanti 2026	TVSA, TVSA (steam-assisted)		Lewatit		T	GAB	WADST	LDF
Zhang 2025	TVSA		Lewatit		T	GAB	WADST	LDF

Legend: TVSA; TVSA (steam-assisted); TVSA (only steam); Packed bed; Mixed reactor; Structured contactor; Monolith; Chemi-sorption; Physi-sorption

Here, we address this question through a multi-model analysis by integrating weather-dependent performance data from seven solid-sorbent DAC models into an otherwise consistent energy system framework. We evaluate the impact of weather year variability as well as model choice and show that CO_2 capture costs, siting preferences and cost-optimal system design most strongly depend on the process representation. Furthermore, we trace part of the resulting variation to individual process-level assumptions through controlled comparisons and evaluate future pathways for technology development. More broadly, our analysis highlights the importance of examining how emerging technologies are represented when system-level assessments are used to inform technology deployment.

Tracing DAC representation to system-level outcomes

The seven solid-sorbent DAC models chosen for this analysis span different process-model representations from literature, which vary in sorbent properties, process configurations, operating conditions and modelling assumptions. A comparison demonstrates that weather-dependent performance, while showing broadly similar trends, varies in magnitude and sensitivity to ambient conditions across representations (Figure 1).

Heat demand generally increases with relative humidity because greater water co-adsorption increases the energy required for regeneration. Electricity demand tends to increase with temperature as decreasing sorbent working capacity requires greater air throughput (i.e., increased cycles) to capture the same amount of CO_2, thereby increasing vacuum and fan work requirements. Productivity decreases correspondingly. Relative humidity can additionally affect productivity through differences in adsorption behavior under dry and humid conditions[35]. However, even these qualitative responses are not universal: in the model of Wiegner et al.[11], for example, all three performance indicators are predominantly influenced by temperature. Additionally, models that predict similar general trends can differ substantially in the magnitude of their response. At approximately 30 °C and 90% relative humidity, for example, the Cai model[28] predicts a heat demand of around 18 MWh t_{CO2}^{-1}, compared with only around 4.5 MWh t_{CO2}^{-1} for Jajjawi[12] —a fourfold difference under identical ambient conditions (more explanation in Supplementary Note 1).

To assess how these differences propagate to the system level, we combine each DAC representation with hourly weather conditions across 20 locations and integrate the resulting energy demand and relative productivity time series into an otherwise consistent energy system model (see Methods). The locations are selected based on weather conditions relevant to DAC operation (temperature and relative humidity) and renewable energy supply characteristics (full load hours of wind and open-field PV plants). Next, we minimize total system cost by jointly optimizing the installed capacities of DAC, renewable generation and energy-storage technologies and their hourly operation. The system is optimized for individual weather years and across ten weather years simultaneously to assess both interannual variability and a system design robust to different weather conditions. By varying only the DAC performance data under otherwise identical conditions, differences in system outcomes can be attributed to DAC representation and its interaction with climate and renewable-resource conditions. The system boundary includes the DAC unit and all required energy infrastructure but deliberately excludes downstream CO_2 processing and life-cycle emissions, thereby focusing the comparison on differences arising from the representation of the capture process itself (see Methods).

Model induced uncertainty dominates interannual weather variability

Using ten years of weather data (2010-2019), we evaluate the influence of DAC model choice and weather year on predicted DAC performance (Figure 2). Overall, annual-average DAC performance (Figure 2a-c) is relatively insensitive to the weather year. Across all locations, interannual variations in heat and electricity demand are model-dependent and range from 1.6-14% and 0.7-8%, respectively, relative to the grand mean. The influence can be larger for specific models and climatic conditions: at a hot-dry location, for instance, the average yearly heat demand of the Jajjawi model differs by 41% between 2015 and 2018. This pronounced variation reflects the model's sensitivity under these conditions, where relatively small changes in temperature and relative humidity can strongly affect heat demand (Figure 1).

DAC model choice introduces substantially greater variation. Across all locations and weather years, the average spread among DAC models reaches 131% for heat demand and 159% for electricity demand, with maximum ranges of 216% and 190%, respectively. The magnitude of these differences also varies strongly across locations, with particularly large deviations under hot-humid conditions. Here, the Cai model predicts exceptionally high heat demand (Figure 1), driven by strong water uptake, whereas the other models exhibit a more moderate response. Electricity demand is more consistent across most models, with the Galanti model as an exception, predicting systematically higher values (see Supplementary Note 1 for more discussion). Beyond energy demand, the models also differ substantially in their predicted relative productivity, defined here as the weather-induced deviation in productivity from a model-specific reference value (see Methods). Both the magnitude and direction of these deviations vary across models and climate conditions.

Model choice affects not only the magnitude of predicted DAC performance, but also the relative favorability and ranking of locations, while individual performance indicators may themselves provide conflicting signals. For instance, when comparing hot-humid and hot-dry locations (Figure 2a-c), the Cai model consistently favors hot-dry conditions, predicting lower heat and electricity demand and higher productivity. The Glaser model predicts the opposite, with all three indicators slightly favoring hot-humid conditions. Location favorability can also be ambiguous, as illustrated by the Wiegner model, which predicts higher electricity demand in hot-dry and higher heat demand in hot-humid conditions, with comparable productivity in both. Furthermore, model rankings can vary between different locations within the same climate archetype, reflecting differences in absolute weather conditions and their temporal correlations. For example, at one hot-dry location, Galanti, Jajjawi and Glaser predict higher heat demand than Cai, whereas at another, Galanti predicts the highest heat demand, followed by Cai, Glaser and Jajjawi (Figure 2a, indicated by red square). Some trends, however, remain robust across models: cold conditions favor productivity in six of the seven models (except Rezo) and are also associated with comparatively low electricity demand, while cold-dry conditions additionally result in relatively low heat demand across all models.

Additionally, model choice determines the temporal response of DAC performance, with models predicting contrasting—and sometimes opposing—seasonal and diurnal patterns (Figure 2d, e). At one moderate climate location Wiegner, Glaser and Galanti predict higher summertime heat demand, whereas Sendi and Jajjawi predict higher demand during winter (Figure 2d). Seasonal responses are themselves location-dependent, with some models showing pronounced differences under hot-dry conditions but more closely aligned profiles under cold-dry conditions (Supplementary Figure 8). Diurnal patterns are even more divergent: Cai, Sendi, Rezo and Jajjawi predict lower daytime and higher nighttime heat demand, whereas Glaser, Wiegner and Galanti predict the opposite (Figure 2e). These differences reflect contrasting weather sensitivities, with heat demand in the former group primarily driven by relative humidity and in the latter by temperature. Because temperature generally peaks during the day while relative humidity tends to increase at night, these sensitivities produce opposing diurnal profiles. Finally, temporal patterns further depend on operating choices such as cycle times and steam use, which is further discussed in Supplementary Note 1.

DAC representation alters system-level conclusions

Comparing the resulting levelized cost of DAC (LCOD) across models and locations highlights substantial variation (Figure 3a). The average spread between the lowest and highest model predictions is 71%, corresponding to nearly 852 € t_{CO2}^{-1}. At one location characterized by cold-humid conditions and hybrid PV and wind supply using performance data from the Galanti rather than the Wiegner model more than doubles the LCOD. In comparison, conventional sensitivity analysis around techno-economic parameters captures only a fraction of the uncertainty introduced by the underlying DAC representation. Varying DAC CAPEX by ±50% changes LCOD by only about 27% on average across models and locations (Supplementary Figure 12). While the results are presented for off-grid renewable-energy supply systems in Figure 3, further analyses show similar results for an unrestricted grid-connected DAC system (Supplementary Figure 15).

Beyond model choice, LCOD also varies substantially across climate conditions, whereas differences between renewable-supply conditions within the same climate category are less pronounced. This suggests that, within the resource conditions considered here, climatic suitability is more consequential for DAC system costs than whether electricity is supplied predominantly by PV, wind or a combination of both. Partitioning the total sum of squares across the evaluated climate-resource archetypes supports this observation. DAC model choice accounts for approximately 43% of the observed variation in LCOD, compared with 16% associated with climate conditions and 6% with renewable-supply conditions.

More consequentially, model-dependent differences propagate into opposing conclusions about location favorability. This is illustrated by comparing a location with moderate climate conditions and hybrid wind and PV supply with a hot-dry location supplied exclusively by PV. Using the performance maps from Cai, Galanti, Sendi or Rezo identifies hot-dry with PV supply as the location with lower LCOD, whereas Jajjawi, Glaser or Wiegner lead to the opposite conclusion (Figure 3a). Importantly, these differences cannot be readily inferred from high-level similarities or differences between the underlying process models. Models that appear structurally similar do not necessarily predict similar system-level outcomes, while models with distinct process representations can lead to the same siting conclusion. For example, Jajjawi, Glaser and Wiegner differ in their sorbent materials and contactor designs (Table 1), yet all favor the moderate climate location over the hot-dry one. Conversely, models sharing

several high-level characteristics, such as Jajjawi and Sendi, can exhibit substantially different responses to ambient conditions and consequently lead to different system-level outcomes. The importance of these model-specific responses is also reflected by partitioning the sum of squares: interactions between DAC model and climate account for an additional 26% of the observed variation in LCOD. This sizeable interaction effect demonstrates that the influence of climate cannot be considered independently of the DAC representation, consistent with the strongly model-dependent responses to ambient conditions identified at the process level. Consequently, siting conclusions derived from system-level assessments are generally not robust to the choice of DAC model.

Although our base-case assessment uses robust optimization across ten weather years, results based on individual weather years reveal a comparatively small influence on LCOD but a substantial effect on cost-optimal system design (Figure 3b). For instance, optimal battery and heat-storage capacities can vary by more than 50% depending on the weather year considered. Robust optimization avoids system designs tailored to the specific conditions of an individual year and provides solutions that remain feasible across a broader range of weather conditions. Yet, even when accounting for interannual variability through robust optimization, system design remains strongly dependent on both location and DAC model choice (Figure 3c). Within individual models, cost-optimal battery capacities are generally larger at PV-dominated locations, consistent with the lower full-load hours and stronger daily pattern of PV generation, which favors battery integration. However, DAC model choice can introduce greater variation than these location-specific trends. For example, at a cold-dry, wind-only location, the Galanti model requires more battery capacity than any other model at a cold-humid, PV-only location. Similarly, renewable generation capacity depends on the interaction between DAC representation and local climate conditions, rather than on renewable-resource conditions alone. This model dependence is substantial: to remove 1 Mt_{CO2} a^{-1} at a cold-dry wind-only location, required wind capacity ranges from approximately 0.6 GW with Wiegner to nearly 2.5 GW with Galanti (Figure 3c). Such differences extend beyond capture cost, with potential implications for land requirements and competition for renewable electricity across sectors. Model representation therefore affects not only the economic assessment of DAC, but also the scale and composition of the energy infrastructure required for its deployment.

Interestingly, the DAC unit is generally operated close to full load in all cost-optimal system configurations, with CO_2 capture largely following the weather-dependent relative productivity of each model (Figure 3d and Supplementary Figure 7). Consequently, the contrasting seasonal and diurnal energy-demand patterns identified at the process level (Figure 2d, e) have only a limited influence on optimal DAC operation at the system level. Instead, the energy system is designed and operated to accommodate these temporal variations. This behavior results from the high capital intensity of current DAC systems: adapting energy-supply and storage capacities is more cost-effective than oversizing the DAC unit and curtailing capture during periods of high energy demand or low energy supply. This trend remains even across a broad range of potential future developments (Supplementary Figure 14), suggesting that DAC flexibility is not as important as reducing capital cost.

Future pathways for achieving low capture costs

The large-scale deployment of DAC in future energy systems will depend strongly on the ability of the technology to achieve sufficiently low CO_2 capture costs. Potential improvements include manufacturing scale-up and technology developments to reduce capital costs, with previous studies projecting substantial reductions through technological learning[8,36], approaching an order of magnitude by 2050[8]. Advances in sorbent properties, heat integration and operating strategies could further reduce energy demand[30,34]. However, given the uncertainty surrounding the magnitude and pace of these improvements, we avoid prescribing a single technology-development trajectory and instead identify combinations of CAPEX and energy-demand reductions under which different DAC models achieve defined capture-cost targets (Figure 4).

The robustness of achieving cost targets depends strongly on both the assumed technological improvements and climatic conditions. Moderate cost targets (~500 € t_{CO2}^{-1}) can be achieved across models at favorable locations with moderate reductions in CAPEX and energy demand, whereas conclusions become increasingly model-dependent for more ambitious cost targets and less favorable climates. For instance, at a location with moderate climate conditions, capture costs below 350 € t_{CO2}^{-1} can be achieved across all models at CAPEX of 500 € $(t_{CO2}/a)^{-1}$ and a 50% reduction in energy demand compared to the current

performance maps (Figure 1). Under hot-humid conditions, however, the same technological assumptions lead to different conclusions: Cai and Galanti remain above 350 € t_{CO2}^{-1}, whereas all other models fall below this threshold. Thus, a combination of CAPEX and energy-demand reductions that appears sufficient to achieve a given cost target under one DAC representation may remain insufficient under another. This model dependence persists for more ambitious cost targets, where reaching 200 € t_{CO2}^{-1} or less requires substantial improvements for all models. Given the International Energy Agency's projected 2050 CO_2 prices of around 200-250 $ t_{CO2}^{-1} in its Net Zero scenario[37], economically self-sustaining DAC deployment at scale would pose a substantial challenge for most current solid-sorbent DAC technologies.

Tracing process-model choices to system-level uncertainty

The preceding analyses demonstrated substantial system-level uncertainty arising from alternative DAC representations. To illustrate how such uncertainty can emerge, we perform controlled comparisons that isolate selected process-level choices within otherwise consistent model formulations. Therefore, we consider four examples spanning material selection, parameterization of material behavior, contactor geometry and operating strategy. These controlled comparisons are not intended to exhaustively attribute the differences between the seven DAC models to individual assumptions. Rather, they demonstrate that substantial variation can originate from individual choices at multiple levels of process modeling. Representations that appear broadly similar at a qualitative level can conceal assumptions and design choices that substantially alter predicted DAC performance and system-level conclusions under real-world weather conditions.

One source of technological variability is the choice of sorbent material. Using the Rezo model, we replace APDES with Lewatit while retaining the remaining model formulation to isolate the influence of material choice on the resulting performance maps and performance under real-world weather conditions (Supplementary Figure 5 and Supplementary Methods). Across all locations, this results in an average difference of 12% (7%) in yearly heat (electricity) demand with a maximum heat demand deviation of 34% under cold-dry conditions (Supplementary Figure 10). The climate dependence of these differences illustrates that sorbent choice can alter the relative suitability of different locations[29]. At the system level, these performance differences translate into an average LCOD difference of 12%, corresponding to nearly 200 € t_{CO2}^{-1} across all locations. More strikingly, substantial uncertainty can arise even without changing the technology represented. Using the Galanti model, we retain the same sorbent and process representation but replace the isotherm parameterization of the base configuration[24] with that fitted by Young et al.[21] from alternative measurements (Supplementary Figure 3). This change alone results in average differences of 60% and 56% in annual heat and electricity demand, respectively, and ultimately a 58% difference in LCOD across locations (Supplementary Figure 6 and Supplementary Figure 11).

Importantly, large changes in individual DAC performance indicators do not necessarily translate into correspondingly large system-level effects. Increasing the bed aspect ratio from 0.5 in the Galanti base configuration[24] to 2 decreases annual heat demand by 23% while increasing electricity demand by 119% on average across locations (Supplementary Figure 4 and Supplementary Figure 6). Despite these substantial changes, average LCOD remains nearly unchanged because the reduction in heat demand largely offsets the increase in electricity demand at the system-level. Operating strategy, by contrast, defines a considerably wider envelope of both process- and system-level outcomes. Using the Glaser model, we compare contrasting operating strategies obtained by optimizing cycle times and steam usage for either minimum energy demand or maximum productivity (Supplementary Figure 2). These strategies differ by 428%, 1328% and 234% in heat demand, electricity demand and productivity, respectively, translating into an LCOD difference of 110% (Supplementary Figure 9 and Supplementary Figure 11). Notably, neither process-level objective minimizes system cost: an intermediate strategy balancing energy demand and productivity—which is used in the main analysis in this study—yields the lowest LCOD across the three strategies. As introduced above, operating choices can also change the resulting performance maps from predominantly temperature-dependent to humidity-dependent behavior and thereby reverse diurnal energy-demand patterns (Supplementary Figure 9).

Discussion

Our results demonstrate that the representation of DAC performance can fundamentally shape conclusions drawn from system-level assessments. The observed model dependency extends beyond uncertainty in the magnitude of predicted capture costs, with an average LCOD spread of 71% between DAC models. Different DAC representations can reverse the location favorability, alter the renewable capacity needed by a factor of four, and change whether identical technology-development assumptions are sufficient to achieve future cost targets. System-level conclusions about DAC should therefore be regarded as conditional on the underlying process representation unless their robustness across alternative representations has been demonstrated.

The underlying quantitative differences between DAC representations reflect two distinct categories: technological variability and epistemic uncertainty. In this classification, variability refers to technological differences, i.e., the use of different sorbents, contactors, cycle designs or regeneration strategies. Such variability is intrinsic to the current stage of DAC development, in which multiple technological concepts coexist, and it remains unclear which configurations will ultimately be deployed at scale. Moreover, the individual process models were developed for different purposes, for example to investigate weather-adapted operating strategies[12,29,31] or design parameters[24], introducing further variability in the process configurations represented. Importantly, this technological diversity also provides opportunities to tailor sorbents, process designs and operating strategies to different ambient conditions, potentially improving performance across climates[29]. Although technological convergence may reduce this variability in the future, this manifests as uncertainty in system-level assessments conducted today. Epistemic uncertainty, on the other hand, refers to models representing similar systems but predicting different outcomes, for example due to using different parameterizations of thermodynamic and kinetic models based on conflicting measurements. Our controlled comparison illustrates that this distinction is consequential beyond the process level: alternative isotherm parameterizations for the same sorbent result in an LCOD difference of 58%. System-level uncertainty therefore arises not only because the future DAC technology remains unsettled, but also because the real-world performance of individual technologies has not yet been fully observed.

This distinction also affects what can reasonably be concluded from system-level DAC assessments at the current stage of technology development. Specific capture-cost estimates, cost-optimal system design and the relative favorability of locations can depend strongly on the selected DAC representation and should therefore not be interpreted independently of that choice. At the same time, some conclusions persist across a broad range of models. Cold-dry conditions, for example, emerge as favorable across most representations, while high utilization of the DAC unit remains cost-optimal across models. Multi-model comparison can therefore serve not only to quantify model dependence, but also to distinguish robust insights from conclusions that remain conditional on a particular technology representation.

Reducing this dependency requires different responses to technological variability and epistemic uncertainty. Technological variability, in particular, should be addressed explicitly in system assessments by including diverse technology configurations rather than prematurely converging on one. This requires closer integration between disciplines, since system modelers and decision makers usually cannot include material- or process-level differences in their assessments and therefore rely on openly available performance data. By providing harmonized performance data alongside this study, we take a step in that direction. Epistemic uncertainty, in contrast, can be progressively reduced through further research and technology demonstration. However, current process models often rely on material properties and transport parameters derived from laboratory-scale measurements, while validation against transient, scale-relevant process data across representative ambient conditions remains limited. Common measurement and benchmarking standards, together with more comprehensive experimental datasets, could help distinguish uncertainties arising from parameterization and scale-up from those inherent to model structure. Furthermore, shared reference conditions for reporting energy demand, productivity and nominal capture capacity would facilitate comparison across models. Public research and testing infrastructure can support these efforts by generating transparent benchmark datasets and validating process models under consistent, scale-relevant conditions.

Our findings contribute to a broader discussion of how system-level conclusions depend on modelling choices. Earlier studies have shown that differences between energy system models can exceed differences between scenarios, and that modeling assumptions such as spatial resolution can substantially alter deployment outcomes[38,39]. We extend this perspective by showing that the representation of a single technology can likewise have a major influence on system-level conclusions. This may extend to other technologies, for example through wind-turbine power curves, building-specific heat loads, or electrolysis part load characteristics. More broadly, such effects are relevant wherever system assessments rely on simplified representations of

technologies whose design and performance remain uncertain or variable. Robust assessments therefore require transparency about technology assumptions and, where feasible, evaluation of alternative representations.

To conclude, we provide the following recommendations. System-level DAC assessments should account for local climatic conditions, as temperature and relative humidity have substantial influence across all solid-sorbent DAC technologies. At the same time, these system-level assessments should consider uncertainty and variability in the underlying DAC performance model and preferably show the solution space across different models. Decision-makers should therefore be particularly cautious when conclusions on favorable locations or expected costs are supported by only a single process model. This is also relevant when detailed system-level results are translated into the more aggregated representations of DAC used in IAMs. As these models support many of the mitigation pathways assessed by the IPCC, adequately representing the technological and regional uncertainty surrounding DAC is important for developing a more robust picture of where, when, and at what cost DAC could contribute to climate-change mitigation.

Methods

Our overall methodology follows a three-step approach that links process-level DAC representations to system-level outcomes (Figure 5). First, performance maps are obtained from published literature or generated from DAC process models and harmonized with respect to units and system boundaries where necessary. Second, these performance maps are combined with hourly resolved weather data for selected locations to derive time series of DAC energy demand and relative productivity. Third, the resulting DAC time series are integrated into an off-grid energy system model together with location-specific time series of PV and wind availability. By varying the underlying DAC representation while retaining the energy system framework and techno-economic assumptions, we isolate how differences in process-level performance propagate to system-level costs, operation and design. More broadly, this workflow represents a technology-assessment framework that connects process modelling, meteorological analysis and energy system optimization (Figure 5).

Derivation of harmonized performance maps

We use seven solid-sorbent DAC models and their corresponding performance maps to quantify how process representation influences system-level outcomes. All models represent DAC systems based on amine-functionalized sorbents. Weather-dependent performance data for two models have been published alongside the corresponding studies[11,28], while Sendi et al.[9] and Jajjawi et al.[12] provide their performance maps as contributions to this study. In addition, we generate performance maps from three further published models (Glaser, Galanti, Rezo)[24,29,31]. For consistency, all performance maps are evaluated for cyclic steady-state conditions. Details on the derivation of these performance maps are provided in the Supplementary Methods. For these three models, we additionally perform controlled variations of selected process-level choices, including sorbent material, isotherm parameterization, bed geometry and operating strategy. These variations are used to isolate how individual modelling and design choices affect predicted DAC performance and subsequently propagate to system-level outcomes. The performance maps are shown in Figure 1.

Two aspects require harmonization before the performance maps can be compared consistently. First, the range of ambient conditions covered by the individual models differs considerably, particularly with respect to temperature. Cai et al.[28] evaluate performance down to -33 °C, whereas the performance data from Wiegner et al.[11] extend only to 1 °C. Following Sendi et al.[9], we impose a common minimum operating temperature of -15 °C across all models. For models without performance data extending to -15 °C, performance below the lowest available temperature is held constant at the value of the lowest available data point. This approach enables a comparison without introducing additional uncertainty due to different shut-off conditions.

Second, a common definition of relative productivity is required to translate weather-dependent DAC performance into the energy system model. Relative productivity determines the fraction of installed DAC capacity that can be utilized under given ambient conditions and is conceptually analogous to the weather-dependent capacity factor of renewable energy technologies, such as wind turbines[13]. For instance, a DAC plant operated in a hot and dry climate might not be able to capture the amount of CO_2 it has been designed for, i.e., the nominal capacity. However, no common convention currently exists for the ambient conditions or

absolute productivity at which nominal DAC capacity—and consequently specific CAPEX expressed per unit of annual capture capacity—is defined. To enable a consistent comparison, we define reference conditions of 20 °C and 50% relative humidity and normalize the productivity of each model individually to its predicted productivity at these conditions. Installed DAC capacity therefore represents the nominal annual CO_2 capture capacity of each model at the common reference conditions, while relative productivity captures model-specific deviations from this capacity as ambient conditions change[13]. Importantly, this normalization preserves differences in the weather sensitivity of productivity but deliberately excludes differences in CAPEX that could arise from differences in absolute productivity between models. Although absolute productivity is expected to influence equipment sizing and investment cost[40], no established relationship exists that would allow these differences to be translated consistently into model-specific CAPEX values across the process configurations considered. We therefore apply consistent specific CAPEX assumptions across models and isolate the influence of their weather-dependent performance.

Finally, all DAC performance maps are harmonized to represent the capture process only, excluding subsequent CO_2 conditioning and compression. For the performance maps created in this study (Glaser, Rezo, Galanti), we directly exclude compression energy from the energy demand. Furthermore, the original performance data from Sendi et al.[9] includes CO_2 compression and associated heat integration. To align the system boundary with the other models, we therefore subtract the electricity demand associated with CO_2 compression and explicitly account for the sensible heat required for steam preheating, which is supplied through waste-heat recovery from compression in the original model. These preprocessing steps and their rationale are described in detail in our previous study[13]. All underlying performance data, harmonization procedures and generated time series are made openly available through a zenodo repository (see Data Availability).

Location selection and time series generation

To evaluate the influence of real-world weather conditions, we select 20 locations geographical representing predefined archetypes relevant to both DAC performance and renewable-energy supply. The archetypes are derived from an analysis of global ERA5 weather data[41] for 2018, which represents an average year for renewable-energy generation[42]. Following Sendi et al.[9], we define five climate archetypes based on annual-average temperature and relative humidity. Cold and hot locations have average temperatures below 10 °C and above 25 °C, respectively, while dry and humid locations have average relative humidities below 55% and above 80%, respectively. Moderate locations are characterized by average temperatures between 10 and 20 °C and relative humidities between 55% and 75%. Combining these criteria yields five climate archetypes: cold-dry, cold-humid, hot-dry, hot-humid and moderate. Renewable-resource archetypes are defined based on the global distributions of PV and wind full-load hours (FLH). PV locations have at least 2200 PV FLH for single-axis tracking systems and no wind supply is modeled, whereas wind locations have at least 2900 wind FLH and no modeled PV supply option. Furthermore, we include two hybrid archetypes to account for the variability in resource conditions: Good hybrid locations combine at least 2000 PV FLH and 2900 wind FLH, while moderate hybrid locations have 1400-2200 PV FLH and 1300-2800 wind FLH. Combining the five climate and four renewable-resource archetypes results in 20 climate–resource combinations. Hundreds of locations globally satisfy these archetype definitions (Figure 5b). Because our objective is not to estimate capture costs at specific geographic locations, but to systematically compare DAC representations across varying climate and renewable-resource conditions, we randomly sample one location from each archetype. The resulting 20 locations and their characteristics are provided in Supplementary Table 2.

Both, the renewable energy time series for wind and PV plants, as well as the time series for DAC units, are derived using open-source workflows from ETHOS.RESKit[43]. These workflows combine weather data with technology characteristics to derive input time series for energy system models. A detailed description of the workflows used to generate time series data for wind and PV can be found in previous works[44,45] and the GitHub repository[43]. DAC time series are obtained by mapping the harmonized performance maps described above to the corresponding hourly ambient temperature and relative humidity.

Techno-economic optimization

To evaluate how alternative DAC representations propagate to the system level, we use an off-grid energy system model comprising onshore wind, single-axis tracking open-field PV (OFPV), a heat pump, an electric boiler, battery electricity storage, thermal storage and the DAC unit. The model is implemented using the open-source energy system optimization framework ETHOS.FINE[46,47] and minimizes total annual cost while respecting constraints such as energy and mass conservation or hourly capacity factors. Optimization variables include the installed capacity of each component and its hourly operation. The weather-dependent DAC time series determine the hourly energy requirements of DAC and constrain CO_2 capture according to the relative productivity within the energy system model. Specifically, DAC operation in each hour is limited by the installed nominal capture capacity multiplied by the corresponding relative productivity. DAC operation is assumed to be fully flexible, motivated by the modularity of solid-sorbent DAC plants, which is expected to enable operation integrated with intermittent renewable energy supply[48]. A fixed annual CO_2 capture quantity of 1 Mt_{CO2} a^{-1} is imposed. Because the optimization problem is linear and no binding upper limits on technology deployment are imposed, system capacities and costs scale linearly with the CO_2 capture target.

We use two approaches to assess the robustness of the results presented in this paper. First, we optimize a single system design against ten years of hourly weather data. Installed capacities are shared across all weather years, while operation is optimized separately subject to the conditions of each year[46]. This parallel multi-year formulation ensures operational feasibility across the full set of weather years and avoids tailoring installed capacities to the conditions of a single year. To quantify the influence of weather-year selection, we additionally optimize each of the ten weather years individually and compare the resulting costs and system designs with the weather-robust solution.

Second, to assess whether the observed model dependence is specific to the off-grid renewable-energy system, we additionally evaluate all DAC representations at the same 20 locations assuming unrestricted electricity supply at a fixed price of 140 € MWh^{-1} (corresponding to the Q2 2026 global average business electricity price[49]). Wind and solar PV are excluded from the energy system model, while all DAC-related assumptions are retained from the main analysis. Because renewable-resource conditions no longer differentiate locations, the four locations originally selected for each renewable supply category provide four independent weather profiles within each climate category.

Techno-economic assumptions are held constant across all DAC models and locations and are summarized in Table 2. A discount rate of 8% is applied throughout. Consequently, differences in optimized system costs, capacities and operation arise solely from the location-specific renewable-resource conditions and weather-dependent DAC performance, enabling a controlled comparison of the influence of DAC representation.

Table 2: Techno-economic parameters used for current and future (2050) assessments. All values have been inflation adjusted and converted to 2024€ using the harmonized consumer price index of the European central bank[50].

Technology	Capex	Fixed Opex (% of Capex)	Economic Lifetime	Further Aspects
DAC	7473 €/(t/a)[19]	4%[19]	20 a[51]	Model-dependent energy demand and relative productivity
Single-axis OFPV	1529 €/kW[52] 700 €/kW (future)[52]	1.4%[52] 1.8%[52]	30 a[52]	Time series simulated using ETHOS.RESKit[43]
Onshore Wind	1608 €/kW[52] 1143 €/kW (future) [52]	2%[52] 2.3%[52]	30 a[52]	Time series simulated using ETHOS.RESKit[43]
Electric Boiler	151 €/kW[53]	0.4%[53]	20 a[53]	
Heat pump	795 €/kW[53] 681 €/kW (future)[53]	0.5%[53] 0.4%[53]	25 a[53]	Ambient air temperature dependent coefficient of performance using an upper temperature of 100 °C and a second law efficiency of 50%
Battery	332 €/kWh[54] 170 €/kWh (future)[54]	2.5%[54]	15 a[54]	Charge-, discharge and self-discharge efficiencies: 96%/96%/0.24%/h[54]
Heat storage	22 €/kWh[55]	0.9%[54]	20 a[54]	Charge-, discharge and self-discharge efficiencies: 98%/98%/0.04%/h[54]

Limitations

This study isolates the uncertainty introduced into system-level DAC assessments by process-model representation and weather-year selection. Accordingly, techno-economic assumptions such as CAPEX, OPEX and financing conditions are held constant across locations and models rather than varied spatially. The resulting capture costs should therefore not be interpreted as comprehensive estimates for individual deployment locations, but as a consistent basis for quantifying differences arising from DAC representation and weather conditions. Our assessment is restricted to solid-sorbent DAC given its strong dependency on ambient conditions and the various available process models in scientific literature.

The system boundary is limited to CO_2 capture and the energy infrastructure required for DAC operation. Subsequent CO_2 conditioning, transport, storage or utilization are not considered. Similarly, we assess gross capture costs rather than net CO_2 removal costs. Accounting for net removal would require consideration of spatially varying upstream emissions associated with energy and infrastructure provision, introducing additional sources of variation beyond the scope of the present representation comparison. The performance maps were generated with the operating strategies of the original studies, which range from fixed cycles to energy-minimizing and trade-off strategies. Our controlled comparison shows that the operating strategy alone can alter system-level cost substantially. Therefore, the spread we attribute to DAC representation reflects differences not only between the mathematical model formulations but also of operating strategies, design decisions and technological variability, highlighting the large decision space rather than isolating the individual aspects.

The selected locations represent contrasting climate-resource archetypes rather than the global distribution of potential DAC sites. Because only one location is sampled per archetype, results should not be interpreted as representative cost estimates for entire climate classes. The location set instead provides controlled, real-world weather conditions for evaluating the sensitivity of system-level conclusions to DAC representation.

Finally, our analysis does not aim to assess the accuracy or suitability of individual DAC process models. Given the limited availability of experimental validation data at representative process scales and operating conditions, identifying the most realistic model is currently not feasible. Instead, our study quantifies how differences between existing DAC representations propagate into system-level assessments, without judging their relative validity.

Declarations

Acknowledgements

This work was supported by the Helmholtz Association under the program “Energy System Design”. H.W. appreciates funding received from the NETs@Helmholtz Research School. M.D. appreciates funding received by the projects ‘Helmholtz-Climate-Initiative’ (HI-CAM) and ‘A Comprehensive Approach to Harnessing the Innovation Potential of Direct Air Capture and Storage for Reaching CO2-Neutrality’ (DACStorE, Grant Agreement Number KA2-HSC-12), which are funded by the Initiative and Networking Fund of the Helmholtz Association. T.T. appreciates the funding received by the Swiss State Secretariat for Education, Research and Innovation (SERI), project ‘UPTAKE’, SBFI No. 23.00212. V.B. acknowledges funding provided by the Swiss State Secretariat for Education, Research and Innovation (SERI) under the Horizon Europe project UPTAKE (grant agreement no. 101081521).

Author contributions

H.W. developed the methodology and software, conceptualized the study, performed the analysis, wrote the original draft and visualized the results; M.Gl., M.Ga. and D.R. simulated DAC models and provided the performance data; T.T. contributed to the original draft; T.T., S.T.M. and J.M.W. gave input on both writing and conceptualization; M.Gl., M.Ga., D.R., A.S.J., M.S., M.v.S.A., S.T.M., T.T., T.S., J.M.W., R.M. and H.W. discussed and iterated the results; T.S., J.L., S.T.M. and J.M.W. supervised the work, provided resources and funding acquisition. All authors reviewed the draft and provided feedback.

Declaration of interests

The authors declare no competing interests.

Data Availability

All optimization results and source data for the figures are provided in a zenodo repository. The repository also contains all input time series data to reproduce the analyses.

Code Availability

The frameworks required to reproduce this study are available open source. Weather-dependent simulations of direct air capture plants and heat pumps were performed using ETHOS.RESKit[43] (https://github.com/FZJ-IEK3-VSA/RESKit), while regional energy system models were implemented using ETHOS.FINE[46] (https://github.com/FZJ-IEK3-VSA/FINE). All model parameters required to reproduce the analyses are provided in the manuscript, Supplementary Information and the corresponding zenodo repository.

Declaration of generative AI and AI-assisted technologies in the writing process

During the preparation of this work the author(s) used ChatGPT and DeepL in order to improve the language of the manuscript. After using this tool/service, the author(s) reviewed and edited the content as needed and take(s) full responsibility for the content of the publication.

References

1. Ganti, G.*; et al.* Evaluating the near- and long-term role of carbon dioxide removal in meeting global climate objectives. *Commun Earth Environ* **5** (2024).
2. Reisinger, A.*; et al.* Overshoot: A Conceptual Review of Exceeding and Returning to Global Warming of 1.5°C. *Annual Review of Environment and Resources,*185–217 (2025).

3. Riahi, K.*; et al.* Mitigation Pathways Compatible with Long-term Goals. In *Climate Change 2022 - Mitigation of Climate Change*; Intergovernmental Panel on Climate Change, Ed.; Cambridge University Press, 2022; pp 295–408.
4. Tavoni, M.*; et al.* Implications of overshoot for climate mitigation strategies. *Nat. Clim. Chang.* **16,** 261–272 (2026).
5. Socolow, R.*; et al. Direct Air Capture of CO2 with Chemicals: A Technology Assessment for the APS Panel on Public Affairs*, 2011. https://res.cloudinary.com/apsphysics/image/upload/v1698255780/Direct-Air-Capture-of-CO2-with-Chemicals_snams5.pdf.
6. Lackner, K. S. Capture of carbon dioxide from ambient air. *Eur. Phys. J. Spec. Top.* **176,** 93–106 (2009).
7. House, K. Z.; Baclig, A. C.; Ranjan, M.; van Nierop, E. A.; Wilcox, J.; Herzog, H. J. Economic and energetic analysis of capturing CO2 from ambient air. *Proceedings of the National Academy of Sciences of the United States of America* **108,** 20428–20433 (2011).
8. Fasihi, M.; Efimova, O.; Breyer, C. Techno-economic assessment of CO2 direct air capture plants. *Journal of Cleaner Production* **224,** 957–980 (2019).
9. Sendi, M.; Bui, M.; Mac Dowell, N.; Fennell, P. Geospatial analysis of regional climate impacts to accelerate cost-efficient direct air capture deployment. *One Earth* **5,** 1153–1164 (2022).
10. Sendi, M.; Bui, M.; Mac Dowell, N.; Fennell, P. Geospatial techno-economic and environmental assessment of different energy options for solid sorbent direct air capture. *Cell Reports Sustainability* **1,** 100151 (2024).
11. Wiegner, J. F.; Grimm, A.; Weimann, L.; Gazzani, M. Optimal Design and Operation of Solid Sorbent Direct Air Capture Processes at Varying Ambient Conditions. *Ind. Eng. Chem. Res.* **61,** 12649–12667 (2022).
12. Jajjawi, A. S.; Wenzel, H.; Harzendorf, F.; Weinand, J. M.; Stolten, D.; Peters, R. Weather-dependent direct air capture process modeling for techno-economic assessments. *Energy Conversion and Management* **351,** 121003 (2026).
13. Wenzel, H.; Harzendorf, F.; Okosun, K.; Schöb, T.; Weinand, J. M.; Stolten, D. Weather conditions severely impact optimal direct air capture siting. *Advances in Applied Energy* **19,** 100229 (2025).
14. Kirppu, H.; Rämä, M.; Pursiheimo, E.; Koponen, K.; Lindroos, T. J. District heating with negative emissions – direct air carbon capture and storage combined with small modular reactors. *Carbon Capture Science & Technology* **17,** 100533 (2025).
15. Zhang, Z.; Miao, Y.; Liu, S.; Gan, Z.; Yu, L. Multi-dimensional process optimization of temperature-vacuum swing adsorption for CO2 capture from humid air. *Energy* **334,** 137733 (2025).
16. Postweiler, P.; Engelpracht, M.; Rezo, D.; Gibelhaus, A.; von der Assen, N. Environmental process optimisation of an adsorption-based direct air carbon capture and storage system. *Energy Environ. Sci.* **17,** 3004–3020 (2024).
17. Rezo, D.; Postweiler, P.; Engelpracht, M.; Meuleneers, L.; von der Aßen, N. A method for siting adsorption-based direct air carbon capture and storage plants for maximum CO2 removal. *Carb Neutrality* **3** (2024).
18. Okosun, K.*; et al.* Global strategic deployment of Direct Air Capture technologies. *International Journal of Greenhouse Gas Control* **155,** 104743 (2026).
19. Terlouw, T.; Pokras, D.; Becattini, V.; Mazzotti, M. Assessment of Potential and Techno-Economic Performance of Solid Sorbent Direct Air Capture with CO2 Storage in Europe. *Environmental science & technology* **58,** 10567–10581 (2024).
20. Jung, H.; Kim, K.; Jeong, J.; Jamal, A.; Koh, D.-Y.; Lee, J. H. Exploring the impact of hourly variability of air condition on the efficiency of direct air capture. *Chemical Engineering Journal* **508,** 160840 (2025).
21. Young, J.; García-Díez, E.; Garcia, S.; van der Spek, M. The impact of binary water–CO 2 isotherm models on the optimal performance of sorbent-based direct air capture processes. *Energy Environ. Sci.* **14,** 5377–5394 (2021).
22. Schellevis, H. M.; La Combé, J. D. de; Brilman, D. W. F. Optimizing direct air capture under varying weather conditions. *Energy Adv.* **3,** 1678–1687 (2024).
23. Schellevis, H. M.; van Schagen, T. N.; Brilman, D. Process optimization of a fixed bed reactor system for direct air capture. *International Journal of Greenhouse Gas Control* **110,** 103431 (2021).
24. Galanti, M.; Kaaresvirta, K.; Roghair, I.; van Sint Annaland, M. Purity-constrained TVSA modeling of Lewatit VPOC 1065 for direct air capture: bridging cured thermodynamics, process design and geometrical analysis. *Energy Adv.* **5,** 273–289 (2026).
25. Young, J.; Mcilwaine, F.; Smit, B.; Garcia, S.; van der Spek, M. Process-informed adsorbent design guidelines for direct air capture. *Chemical Engineering Journal* **456,** 141035 (2023).

26. Abdullatif, Y. M.; Sodiq, A.; Al-Ansari, T.; Nassar, N. N.; Amhamed, A. I. Optimizing chemisorption based direct air capture unit efficiency in HVAC systems: A study on the impact of DAC location and adsorption conditions as a response to the climate crisis and indoor air quality. *Energy Conversion and Management* **291,** 117280 (2023).
27. Balasubramaniam, B. M.; Thierry, P.-T.; Lethier, S.; Pugnet, V.; Llewellyn, P.; Rajendran, A. Process-performance of solid sorbents for Direct Air Capture (DAC) of CO2 in optimized temperature-vacuum swing adsorption (TVSA) cycles. *Chemical Engineering Journal* **485,** 149568 (2024).
28. Cai, X.; Coletti, M. A.; Sholl, D. S.; Allen-Dumas, M. R. Assessing Impacts of Atmospheric Conditions on Efficiency and Siting of Large-Scale Direct Air Capture Facilities. *JACS Au* **4,** 1883–1891 (2024).
29. Glaser, M.; Rajendran, A.; McCoy, S. T. How do ambient conditions influence sorbent selection in adsorption-based direct air capture? *Sustainable Energy Fuels* **9,** 4404–4416 (2025).
30. Sabatino, F.; Grimm, A.; Gallucci, F.; van Sint Annaland, M.; Kramer, G. J.; Gazzani, M. A comparative energy and costs assessment and optimization for direct air capture technologies. *Joule* **5,** 2047–2076 (2021).
31. Rezo, D.; Glaser, M.; Postweiler, P.; Engelpracht, M.; von der Assen, N. Control strategies to optimize adsorption-based direct air capture under varying weather conditions. *Applied Energy* **411,** 127578 (2026).
32. Shakouri Kalfati, M.; Abdulla, A. An open-source dynamic model for direct air capture of carbon dioxide using solid sorbents. *Carbon Capture Science & Technology* **17,** 100516 (2025).
33. Ward, A.; Papathanasiou, M. M.; Pini, R. The impact of design and operational parameters on the optimal performance of direct air capture units using solid sorbents. *Adsorption* **30,** 1829–1848 (2024).
34. Ferru, N.; Morgado, N. A.; Bardow, A.; Mazzotti, M. Leveraging the phase change of water for energy efficient direct air capture. *Chemical Engineering Journal* **535,** 175574 (2026).
35. Elfving, J.; Sainio, T. Kinetic approach to modelling CO2 adsorption from humid air using amine-functionalized resin: Equilibrium isotherms and column dynamics. *Chemical Engineering Science* **246,** 116885 (2021).
36. Hanna, R.; Abdulla, A.; Xu, Y.; Victor, D. G. Emergency deployment of direct air capture as a response to the climate crisis. *Nature communications* **12,** 368 (2021).
37. International Energy Agency. *Net Zero Roadmap: A Global Pathway to Keep the 1.5 °C Goal in Reach*. 2023 Update; Paris, 2023. https://iea.blob.core.windows.net/assets/8ad619b9-17aa-473d-8a2f-4b90846f5c19/NetZeroRoadmap_AGlobalPathwaytoKeepthe1.5CGoalinReach-2023Update.pdf.
38. Dekker, M. M.*; et al.* Identifying energy model fingerprints in mitigation scenarios. *Nat Energy* **8,** 1395–1404 (2023).
39. Beiter, P.; Mai, T.; Mowers, M.; Bistline, J. Expanded modelling scenarios to understand the role of offshore wind in decarbonizing the United States. *Nat Energy* **8,** 1240–1249 (2023).
40. van der Spek, M.*; et al.* An ecosystem of carbon dioxide removal reviews - part 1: direct air CO2 capture and storage. *Energy & environmental science* **18,** 9713–9785 (2025).
41. Hersbach, H.*; et al.* The ERA5 global reanalysis. *Quart J Royal Meteoro Soc* **146,** 1999–2049 (2020).
42. International Renewable Energy Agency. *Global hydrogen trade to meet the 1.5°C climate goal: Part III – Green hydrogen cost and potential*, 2022. https://www.irena.org/-/media/Files/IRENA/Agency/Publication/2022/May/IRENA_Global_Hydrogen_Trade_Costs_2022.pdf.
43. Jülich Systems Analysis, Forschungszentrum Jülich GmbH. *ETHOS.RESKit - Renewable Energy Simulation Toolkit*, 2026. https://github.com/FZJ-IEK3-VSA/RESKit.
44. Peña-Sánchez, E. U.*; et al.* Towards high resolution, validated and open global wind power assessments. *Nature communications* **17,** 539 (2026).
45. Winkler, C.*; et al.* Participatory mapping of local green hydrogen cost-potentials in Sub-Saharan Africa. *International Journal of Hydrogen Energy* **112,** 289–321 (2025).
46. Jülich Systems Analysis, Forschungszentrum Jülich GmbH. *ETHOS.FINE - Framework for Integrated Energy System Assessment*, 2026. https://github.com/FZJ-IEK3-VSA/FINE.
47. Klütz, T.*; et al.* ETHOS.FINE: A Framework for Integrated Energy System Assessment. *JOSS* **10,** 6274 (2025).

48. Liu, Y.*; et al.* Addressing solar power curtailment by integrating flexible direct air capture. *Carbon Capture Science & Technology* **14,** 100304 (2025).
49. GlobalPetrolPrices.com. Electricity prices. https://www.globalpetrolprices.com/electricity_prices/ (accessed August 26, 2026).
50. European Central Bank. HICP - Overall index, Euro area (changing composition), Monthly. https://data.ecb.europa.eu/data/datasets/ICP/ICP.M.U2.N.000000.4.INX (accessed July 16, 2025).
51. Wenzel, H.*; et al.* Towards water-conscious green hydrogen and methanol production: A techno-economic review. *Nexus* **2,** 100054 (2025).
52. National Renewable Energy Laboratory. *2024 Annual Technology Baseline*, 2024. https://atb.nlr.gov/electricity/2024/data.
53. Grosse, R.; Christopher, B.; Stefan, W.; Geyer, R.; Robbi, S. *Long term (2050) projections of techno-economic performance of large-scale heating and cooling in the EU*; Publications Office: Luxembourg, 2017.
54. Stolten, D.*; et al. Neue Ziele auf alten Wegen? Strategien für eine treibhausgasneutrale Energieversorgung bis zum Jahr 2045*; Reihe Energie & Umwelt / Energy & Environment No. 577; Schriften des Forschungszentrums Jülich, 2022.
55. Pompei, L.; Nardecchia, F.; Miliozzi, A. Current, Projected Performance and Costs of Thermal Energy Storage. *Processes* **11,** 729 (2023).

Figures

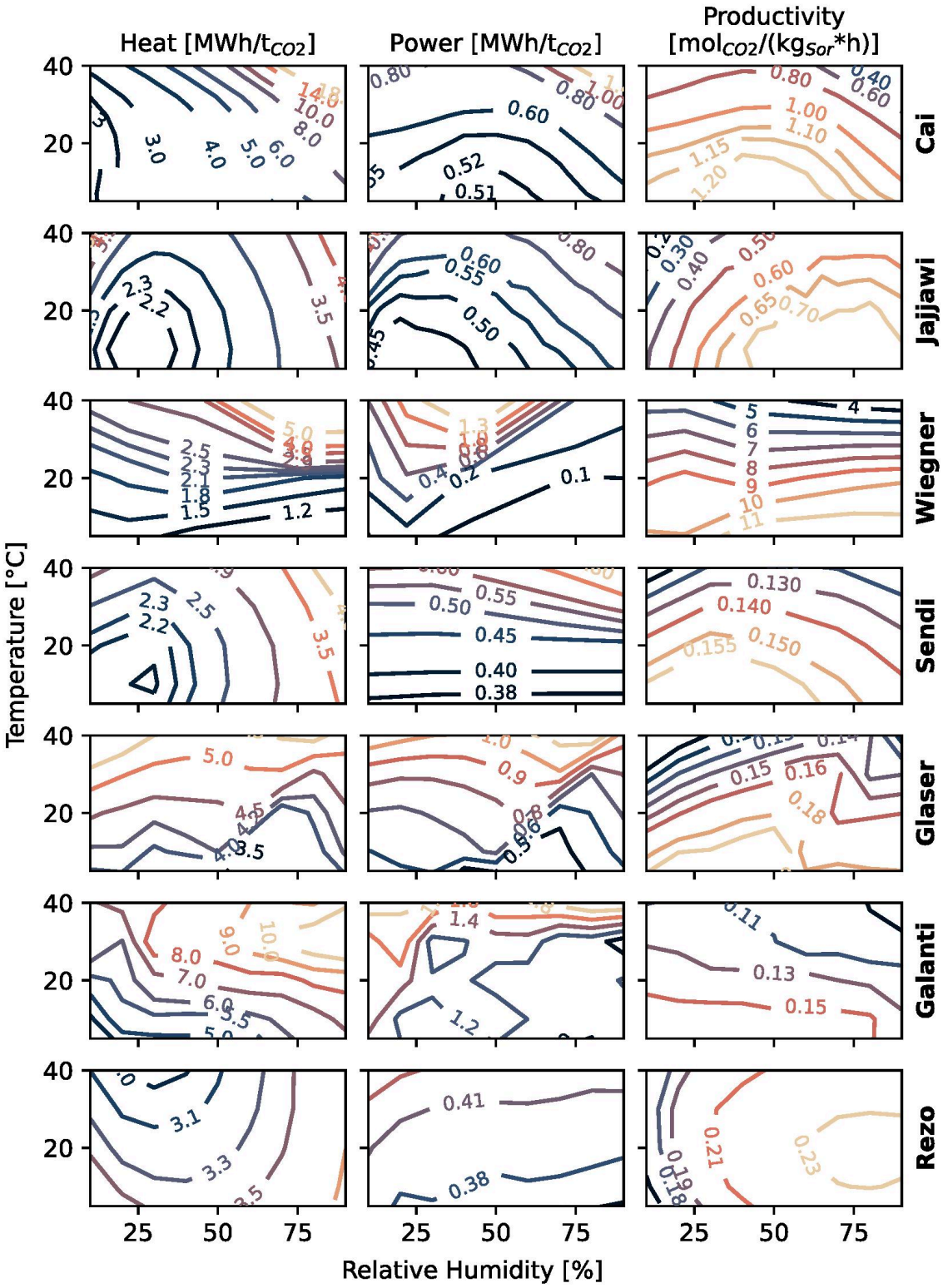


Figure 1

Performance of different DAC process models[9,11,12,24,28,29,31] under varying ambient conditions. The models by Sendi[9], Jajjawi[12] and Galanti employ Lewatit as sorbent, while the Rezo[31] version shown here and Glaser[29] use APDES. Cai[28] uses a proprietary sorbent from Elfing et al.[35] and Wiegner[11] employs exemplary data combined from different sorbents. All models vary in their parameterization, i.e., by using different isotherm and kinetic parameters, transport data or design and operation variables. In particular, the models by Rezo, Galanti and Glaser are optimized for a trade-off between maximum productivity and minimum energy demand, while the Jajjawi model is optimized for minimum energy demand and the other models are not optimized for

weather-adapted behavior. While Cai[28] and Wiegner[11] published the performance data of their models, the data of the other models was available from the authors as a contribution within this collaborative study[9,12] or is explicitly created from the process models in this study[24,29,31] (for more explanation see Supplementary Notes 1). All data is shared in the Supplementary Material. Enlarged versions of the performance maps can be found in Supplementary Figure 1 and Supplementary Figure 16.

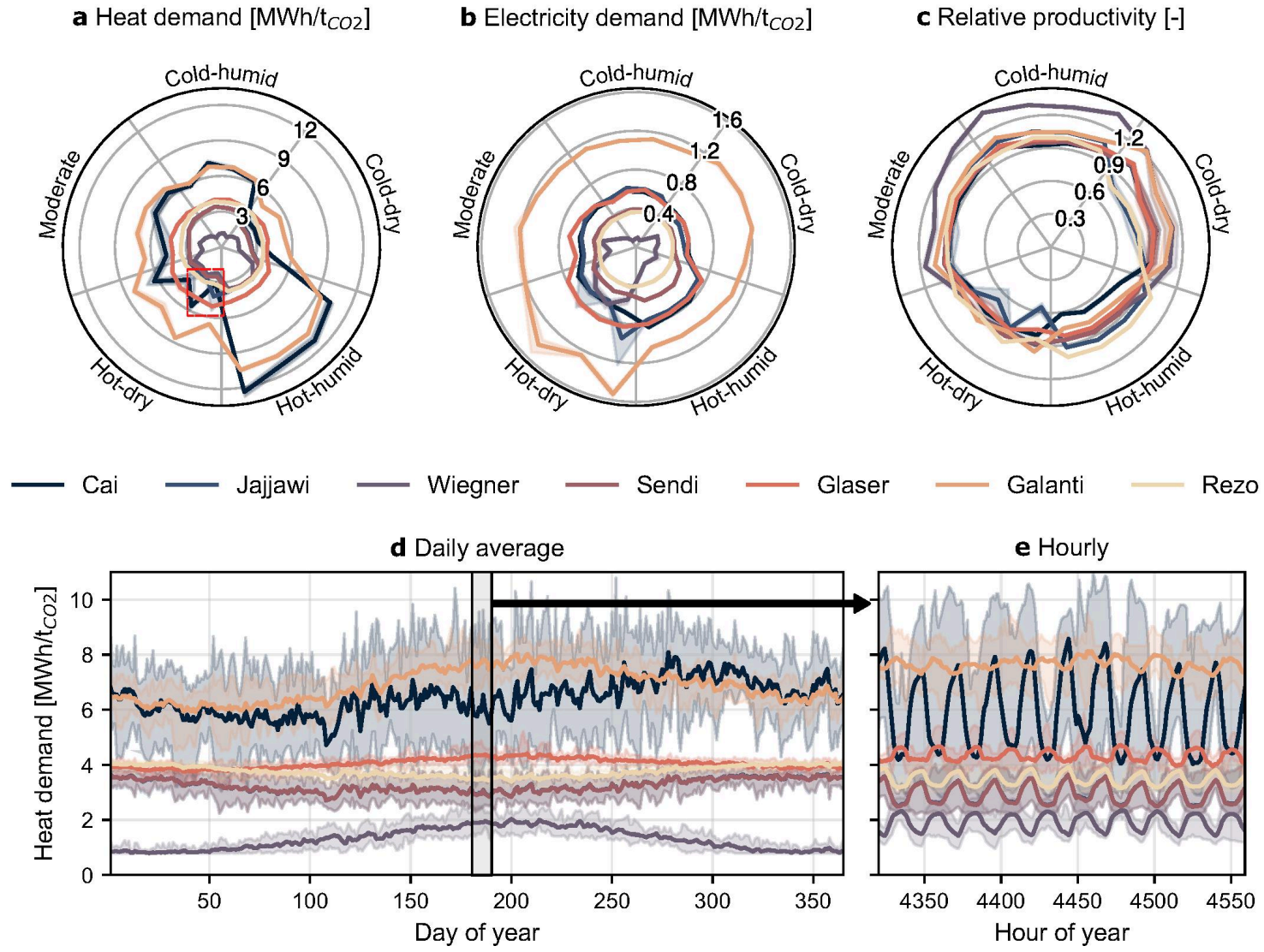


Figure 2

Performance of seven solid sorbent DAC models at various locations for different weather years. The line corresponds to the mean of weather years 2010 to 2019 while the shaded area indicates the variability of different weather years. a-c. Yearly average heat demand, electricity demand and relative productivity. For each climate category, 4 different regions with varying renewable resources are shown (see Methods). Interannual variability is very small, so the transparent area is only visible for some model-climate combinations. d. Daily average heat demand at a location with moderate climate conditions. The models by Jajjawi and Sendi predict nearly the same pattern, resulting in an overlap in this and the following subpanel. e. Hourly heat demand for the days indicated by the grey area in tile d. The hourly time series shown here serve as an input for the energy system model, which then decides at which capacity the DAC unit is operated in each hour, resulting in the plant-level energy demand.

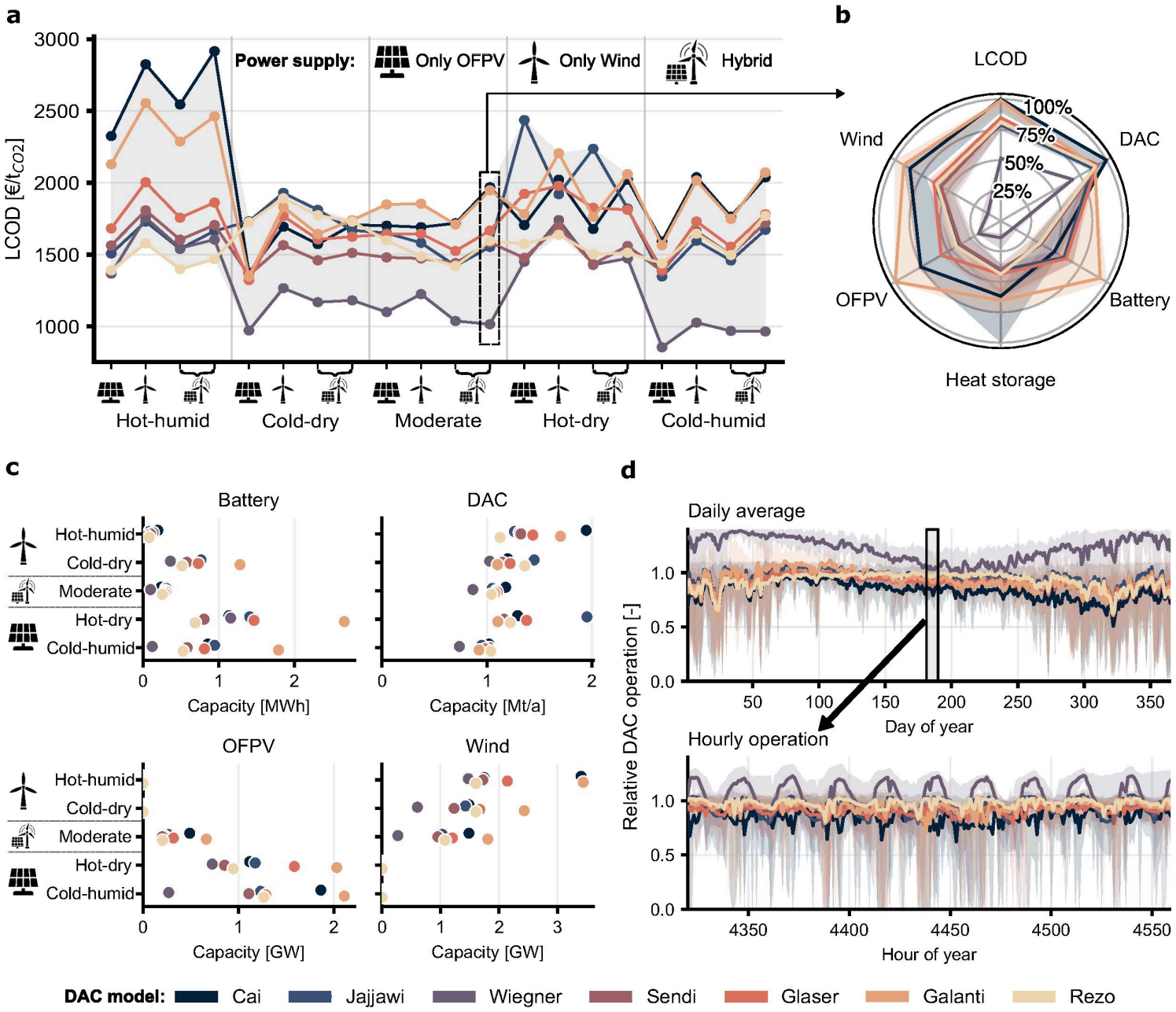


Figure 3

Resulting cost, system design and optimal operation for different DAC models. a. Levelized cost of DAC (LCOD) in different locations grouped by climate conditions and renewable energy supply. For hybrid power supply, two locations with varying full load hours are shown (see Methods). Each dot represents a robust optimization against 10 weather years. b. LCOD and cost-optimal system design variation for one location with moderate climate and hybrid renewable supply depending on model choice and weather year. The line represents the robust optimization while the shaded area represents the optimization results of optimizing each weather year individually. c. Robust optimal system design for an exemplary system to capture 1 Mt a^{-1}. d. Operation relative to the nominal installed capacity of the DAC plant for the robust optimization at a location with moderate climate and hybrid renewable supply. The line is the average across all years while the shaded area represents the operation in different weather years. A relative operation >1 indicates that the productivity of the corresponding model under the prevailing ambient conditions is higher than the defined reference productivity at 20 °C and 50% relative humidity (see Methods). This can result in a lower installed nominal capacity than the actual yearly capture quantity of 1 Mt a^{-1}. Icons by Flaticon.com.

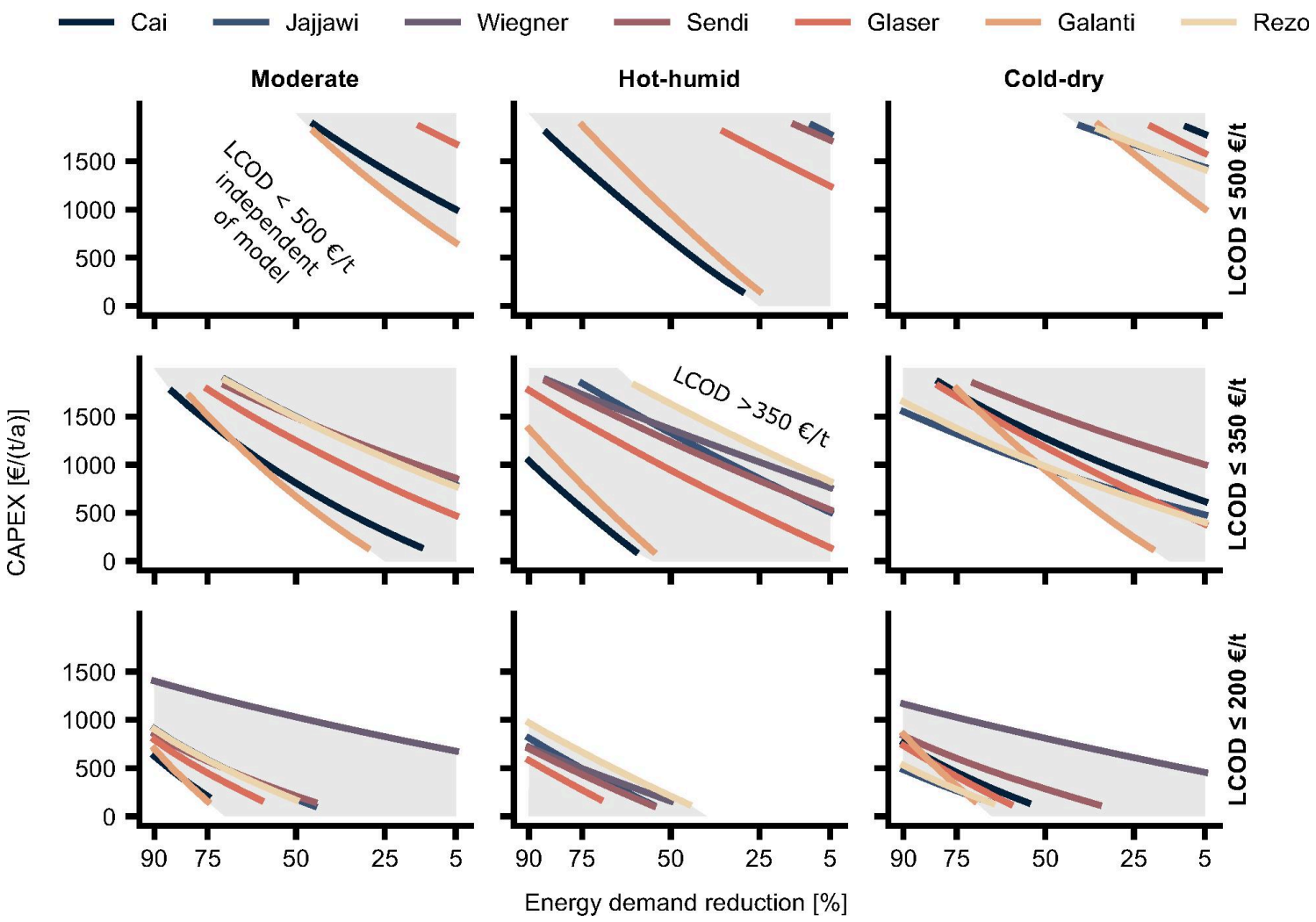


Figure 4

Conditions for future (2050) capture cost below thresholds of 500, 350 or 200 € t_{CO2}^{-1} depending on the model and region. Each line represents the combination of CAPEX and energy demand reductions relative to the current performance maps to achieve capture costs of the threshold under future (2050) energy system assumptions (see Methods). Moving to the lower left of a line means that capture cost below the threshold could be achieved using that model, while moving to the upper right means that the capture cost would be above the threshold. Consequently, the grey area indicates combinations of CAPEX and energy demand reductions where achieving the target cost depends on the model. For reference, current CAPEX in this study are assumed to be at about 7500 €/(t_{CO2}/a)[19] (see Methods).

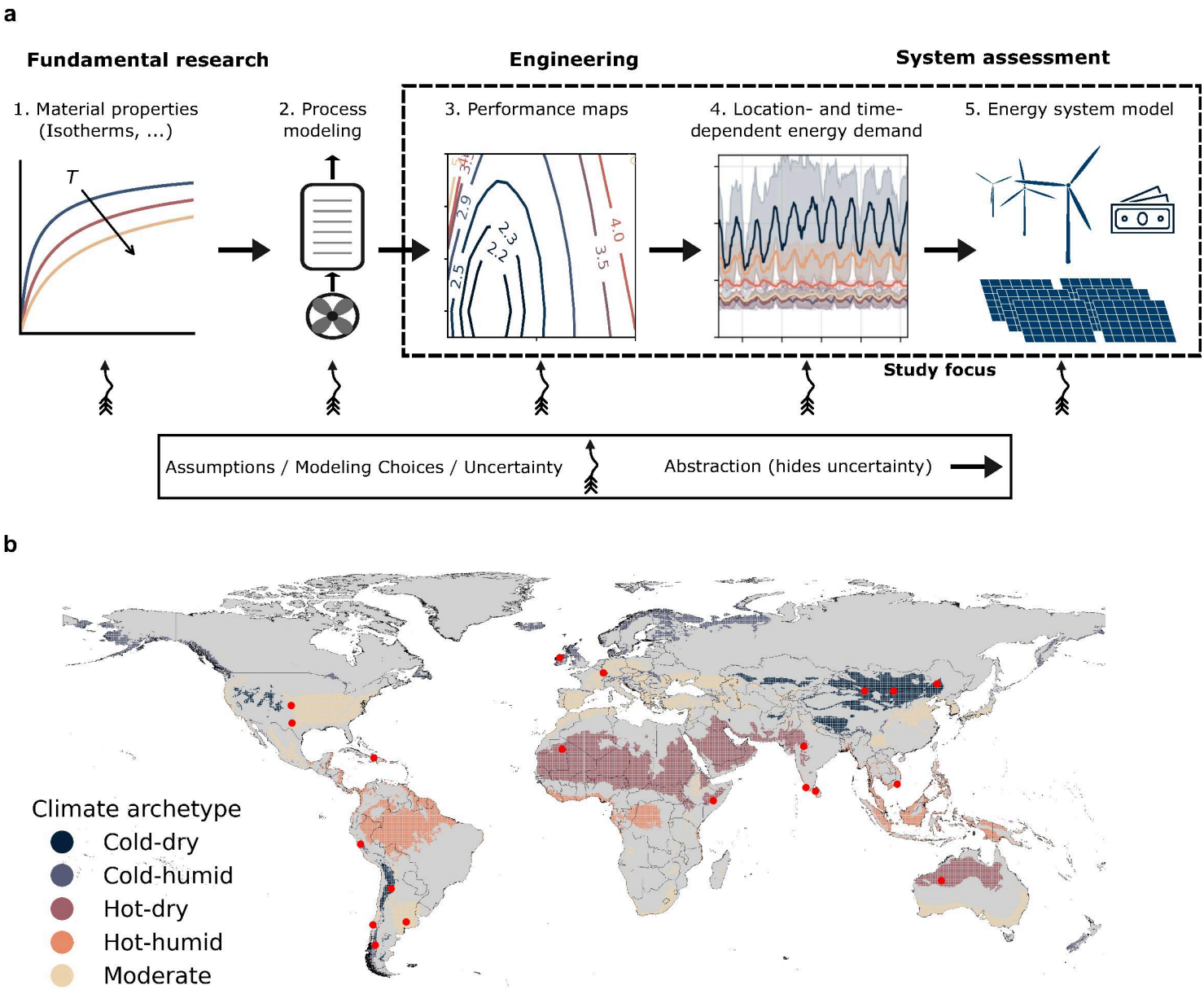


Figure 5

Overview of the methodology. a. General workflow for process-to-system-level technology assessment with DAC specific examples, as applied in this study. In each step, assumptions, modeling choices as well as epistemic uncertainties enter the evaluation and influence the results. While progressing through the technology assessment, abstraction hides this variability and uncertainty. b. Global locations colored by climate conditions. Each of the colored locations also fits within one of the defined renewable-resource conditions. The 20 randomly selected locations for which the assessment has been conducted are highlighted by red dots. Climate and renewable resource conditions for those locations are specified in Supplementary Table 2.

Supplementary Files

This is a list of supplementary files associated with this preprint. Click to download.

- DACModelComparison.xlsx
- DACUncertaintySI.docx